OXFORD Toxicology Research

Toxicology Research, 2020, **9**, 149–157

doi: 10.1093/toxres/tfaa015
Advance Access Publication Date: 28 April 2020
Paper

PAPER

Pyrazinamide enhances lipid peroxidation and antioxidant levels to induce liver injury in rat models through PI3k/Akt inhibition

Yun Xu, Yongfang Jiang and Yi Li*

Department of Infectious Diseases, The Second Xiangya Hospital of Central South University, Changsha, Hunan 410011, China

Correspondence address. Yi Li, Department of Infectious Diseases, The Second Xiangya Hospital of Central South University, No. 139 Renmin Road, Changsha 410011, Hunan, China. Tel: +86 13808489650; E-mail: liyi731128@csu.edu.cn

Abstract

Pyrazinamide (PZA) is an anti-tuberculosis drug known to causes liver injury. phosphatidylinositol-3-kinase/protein kinase B (PI3K/Akt) signaling protects against liver injury by promoting cellular antioxidant defenses and reducing intracellular reactive oxygen species (ROS) and lipid peroxidation. The regulatory mechanisms and functions of PI3K/Akt signaling during the hepatotoxicity of PZA are however not fully understood. Rats were administered PZA or/and the PI3K activator (740Y-P) for 7 days. The levels of serum parameters were examined via standard enzymatic techniques and the pathological status of the liver was confirmed by H & E staining. The levels of lipid peroxidation and antioxidant production were determined using commercial kits. Liver apoptosis was assessed by TUNEL staining. The expression of apoptosis-related proteins and PI3K/Akt signaling were assessed by western blot analysis. PZA treatment significantly increased serum alanine transaminase, aspartate transaminase, gamma-glutamyl transpeptidase and tall bilirubin leading to liver damage in rats. PZA also facilitated lipid peroxidation and suppressed antioxidant defenses. PZA led to apoptotic induction in rat liver cells through the downregulation of Bcl-2 and the upregulation of Bax and caspase-3. PZA also dramatically inhibited PI3K/Akt signaling in rat liver cells. We further verified that PI3K/Akt signaling in response to 740Y-P could attenuate hepatic injury, lipid peroxidation and apoptosis in rat liver cells in response to PZA. We reveal that PZA-induced liver injury in rats occurs through PI3k/Akt signaling, the recovery of which prevents liver injury in rat models.

Key words: pyrazinamide, liver injury, lipid peroxidation, antioxidant system, PI3k/Akt

Introduction

Tuberculosis (TB) is a chronic infectious disease that can endanger public health [1]. TB treatment includes standardized short-course chemotherapy, consisting of combined rifampicin, isoniazid, pyrazinamide (PZA) and ethambutol for 6–8 months [2]. Because of the long-term and high-dose combination of anti-TB drugs, TB patients display different degrees of adverse drug reactions during treatment, among which liver injury is the most common [3, 4]. Indeed, drug-induced liver injury is the main reason for the discontinuation of patients receiving TB treatment [5]. In addition, liver injury can increase patient suffering, delay recovery and endanger the life of patients [6]. In clinical practice, domestic physicians are accustomed to the preventive application of liver protective drugs to prevent the occurrence of anti-TB drug-induced liver injury that have largely failed to reduce the incidence of liver injury [7].

PZA is similar in structure to nicotinamide and can enter cells to kill bacteria [8]. PZA is an irreplaceable first-line

Received: 22 October 2019; **Revised:** 5 March 2020; **Accepted:** 16 March 2020

anti-TB drug recommended by the World Health Organization (WHO) [9] that is a continuous bactericidal drug that kills both vigorous metabolism and static TB bacteria in an acidic environment [10]. PZA can shorten the treatment time of TB patients and has attracted intense research interest [11]. However, the occurrence of adverse reactions caused by PZA are as high as 49.9%, which is significantly higher than other first-line anti-TB drugs including rifampicin (adverse reaction rates = 16.6%) and isoniazid (adverse reaction rates = 11.1%) [12]. The clinical use and patient compliance to PZA are therefore limited.

Studies on methods to improve PZA drug-induced liver injury are urgently required [13, 14]. Liver injury is a major cause of liver disease and death, the mechanisms of which are complex and include intrahepatic immune responses, lipid peroxidation, oxidative stress (OS), lipid membrane damage, mitochondrial dysfunction, cell apoptosis, changes in intracellular ion concentrations and metabolic disorders [15–17]. Further exploration of these mechanism(s) have the potential to alleviate PZA-induced liver injury.

The cellular and molecular mechanisms for drug-induced hepatotoxicity are complex [18]. Phosphatidylinositol 3-kinases (PI3K) specifically catalyze phosphatidylinositol (PI) phosphorylation [19] and activate 3-phosphoinositol-dependent kinase 1 (PDK1) by binding to the PH domain at the N terminus of protein kinase B (Akt). PDK-1 and PDK-2 phosphorylate Thr308 and Ser473 in Akt, respectively [20], and Akt is phosphorylated and becomes activated further regulating target genes [21]. PI3K/Akt signaling has emerged as a crucial signal transduction pathway in cells with significant effects on cell proliferation, survival, apoptosis, metabolism, OS and the immune response [22, 23]. Studies have shown that the PI3K/Akt pathway is closely related to drug-induced liver injury [24–26] but whether PZA-induced liver damage is associated with PI3K/Akt signaling is not fully defined.

In this study, we assessed the influence of different concentrations of PZA on rat liver damage, lipid peroxidation, the antioxidant system and apoptosis. We confirmed the regulatory effects of PZA on the expression of PI3K/Akt in rats and verified that the PI3K/Akt pathway regulates liver injury in response to PZA. These data provide a novel solution to alleviate PZA-induced liver injury to improve patient tolerance during TB treatment.

Materials and Methods

Animals

Sprague Dawley (SD) rats (males, 150–200 g, $n = 70$) were provided by the Animal Experiment Center of the Institute of Radiation Medicine of the Chinese Academy of Medical Science. All animal programs were approved by Animal Experiment Center of the Institute of Radiation Medicine of the Chinese Academy of Medical Science. Prior to the experiments, all the animals were allowed to adapt to the new environment. Feeding conditions free access to water and food, temperature: 20–24°C, humidity: 50–60% and a 12 h light/dark cycle.

Groups

A total of 40 SD rats were randomly divided into 4 groups: control group (SD rats orally administered 4 ml/kg normal saline for 7 days) and 3 PZA groups (SD rats orally administered 0.5 g/kg, 1 g/kg and 2 g/kg PZA for 7 days) [14, 27]. In addition, a total of 30 SD rats were randomly divided into three groups: PZA (SD rats orally administered 2 g/kg PZA for 7 days), PZA + vehicle group (2 g/kg PZA-treated SD rats injected intramuscularly with normal saline), PZA + 740Y-P group (2 g/kg PZA-treated SD rats injected intramuscularly with 740Y-P).

Hepatotoxicity assays

After fasting overnight, SD rats were sacrificed under anesthesia through the intraperitoneal injection of 5% chloral hydrate (200 mg/kg, Sigma-Aldrich). Blood samples were collected from the abdominal vena cava according to standard enzymatic techniques and the levels of serum alanine transaminase (ALT) and aspartate transaminase (AST) quantified. Glutamyl transpeptidase (γ-GT) and tall bilirubin (TBIL) were examined on an automatic biochemical analyzer.

Hematoxylin and eosin (H&E) staining

Liver tissues of rats treated with different concentrations of PZA or/and 740Y-P were isolated and fixed in 4% paraformaldehyde (Sigma-Aldrich, cat. no. P6148). Tissues were dehydrated in a gradient of alcohol and tissues were transparently treated in dimethylbenzene. Tissues were paraffin-embedded and sectioned (5 μm slices). Sections were hematoxylin stained for 5 min and treated with 5% acetic acid for 1 min and eosin for 1 min. After dehydration, sections were added to neutral balsam and images were visualized under a microscope (Nikon, Japan).

Determination of OS markers

Based on the standard procedures, the concentration of thiobarbituric acid reactive substances (TBARS) [28], reactive oxygen species (ROS) [29], glutathione peroxidase (GPx) [30], catalase [31] and glutathione (GSH) were assessed [32].

TUNEL staining

Paraffin-embedded sections were treated with dimethylbenzene for 5 min, anhydrous ethanol, and 95% and 75% ethanol for 3 min. After washing with phosphate-buffered saline (PBS), sections were treated with 20 μg/ml Proteinase K for 15 min. After washing, sections were permeabilized in 0.1% Triton-X and 0.1% sodium citrate and incubated in 0.1% Tween-20 for 30 min. After washing, sections were stained in DNA Fragmentation Imaging Kits (Roche). Images were obtained using a Nikon TE300 microscope (Nikon).

Western blot analysis

Total proteins were isolated from liver tissue using RIPA Lysis Buffer (Vazyme, cat. no. FD008) with PMSF (Solarbio; cat. no. P0100–1.5). Protein concentrations were determined by BCA assay (Beyotime) and equal concentrations were resolved by sodium dodecyl sulfate–polyacrylamide gel electrophoresis and electroblotted onto polyvinylidene fluoride (PVDF) membranes (Amersham). After blocking in 5% non-fat dry milk, membranes were labeled in primary antibodies overnight at 4°C and probed with HRP-conjugated secondary antibodies. Protein bands were visualized on an enhanced chemiluminescence (ECL) detection system (Amersham) following exposure to X-ray film. Antibodies in the study included anti-glyceraldehyde 3-phosphate dehydrogenase (anti-GAPDH) (Abcam; cat no. ab37168), anti-Bax (Abcam; cat no. ab32503), anti-Bcl-2 (Abcam, Cat no. ab32124), anti-caspase-3 (Santa Cruz Biotechnology; cat

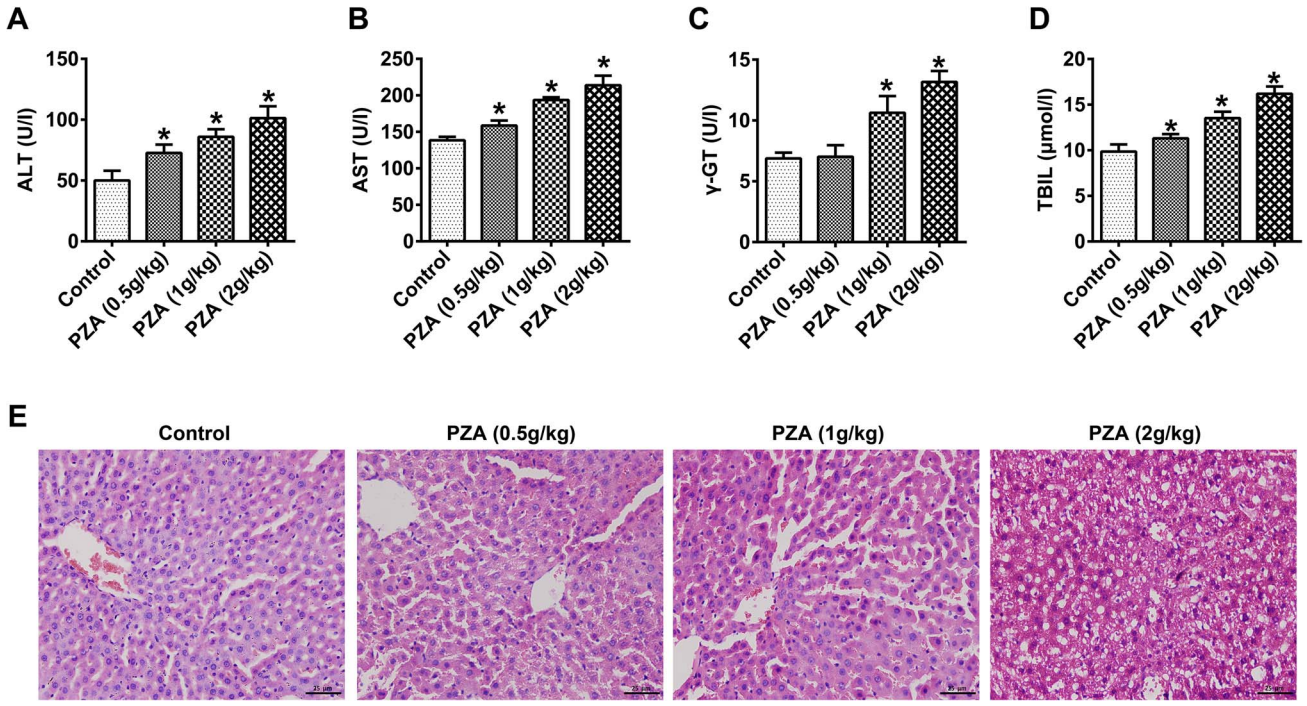

Figure 1: PZA-induced liver injury in rats. Levels of serum parameters including ALT (A), AST (B), γ-GT (C), TBIL (D) were examined in rats treated with 0.5 g/kg, 1 g/kg and 2 g/kg PZA, respectively, *$P < 0.05$ vs. control group. (E) Pathological status of liver injury determined by H&E staining. Magnification, ×200, scale bar = 25 μm.

no. sc-7148), anti-PI3K (Sigma-Aldrich; cat. no. 5295), anti-p-PI3K (Bioworld Technology; cat. no. BS4605), anti-Akt (Cell Signaling; cat. no. 4685) and anti-p-Akt (Cell Signaling Technology; cat. no. 4058s).

Statistical analysis

Data were expressed as mean ± SD from three independent experiments. Data were analyzed on GraphPad Prism Software (Ver. Prism 7) or SPSS 20.0 software. Differences were calculated using one-way analysis of variance followed by Bonferroni post hoc test. $P < 0.05$ and $P < 0.01$ were deemed statistically significant.

Results

PZA-induced liver injury in rats

To identify the influence of PZA on liver injury in rats, rats were orally administered 0.5 g/kg, 1 g/kg and 2 g/kg PZA for 7 days. The assessment of serum parameters showed that ALT, AST, γ-GT and TBIL levels were significantly elevated in PZA treatment groups relative to controls, in a dose-dependent manner ($P < 0.05$, Fig. 1A and D). In addition, H&E staining revealed that, in the control group, the hepatic lobules were clearly structured, hepatic cords were radially arranged, hepatocytes had uniform cytoplasm and the hepatocytes showed no obvious edema and steatosis. In the PZA treatment group, rat liver cells showed edema, cytoplasmic relaxation and obvious ballooning degeneration. In addition, the hepatic cord structures and perisinus space disappeared, the liver was also accompanied by inflammatory cell infiltration, and the degree of liver injury gradually increased with increasing PZA concentrations (Fig. 1E). Our data therefore showed that PZA could facilitate hepatic injury in rats.

PZA enhanced lipid peroxidation and inhibits the antioxidant system of rats

We next examined the impact of PZA on lipid peroxidation and the antioxidant system. Our results confirmed that the levels of lipid peroxidation (TBARS) were significantly enhanced in PZA treatment groups compared to control groups in a dose-dependent-manner ($P < 0.05$, Fig. 2A). Antioxidant assessments showed that the levels of SOD, GPx, catalase and GSH were significantly reduced in the PZA treatment group compared to the control group, with the reductions showing a dose-dependent effect ($P < 0.05$, Fig. 2B and E). These results revealed that PZA could dramatically promote lipid peroxidation and suppress antioxidant defenses in rats.

PZA promotes apoptosis in rat livers

We next assessed the effects of PZA on rat liver apoptosis using TUNEL staining. Figure 3A shows that the apoptotic ratio markedly increased in the PZA treatment group compared to control groups ($P < 0.05$) suggesting that PZA accelerated apoptosis in rat livers. In addition, we explored the mechanisms by which PZA promotes apoptosis. Western blot analysis revealed that Bcl-2 was downregulated, whereas Bax and caspase-3 expression were upregulated in the PZA treatment group versus the control group ($P < 0.05$, Fig. 3B).

PZA downregulates the expression of PI3K/Akt in rat liver

To investigate the mechanisms by which PZA induces liver injury in rats, the expression of components of the PI3K/Akt pathway were assessed by western blot analysis. As shown in Fig. 4, p-PI3K and p-Akt expression were significantly downregulated in PZA

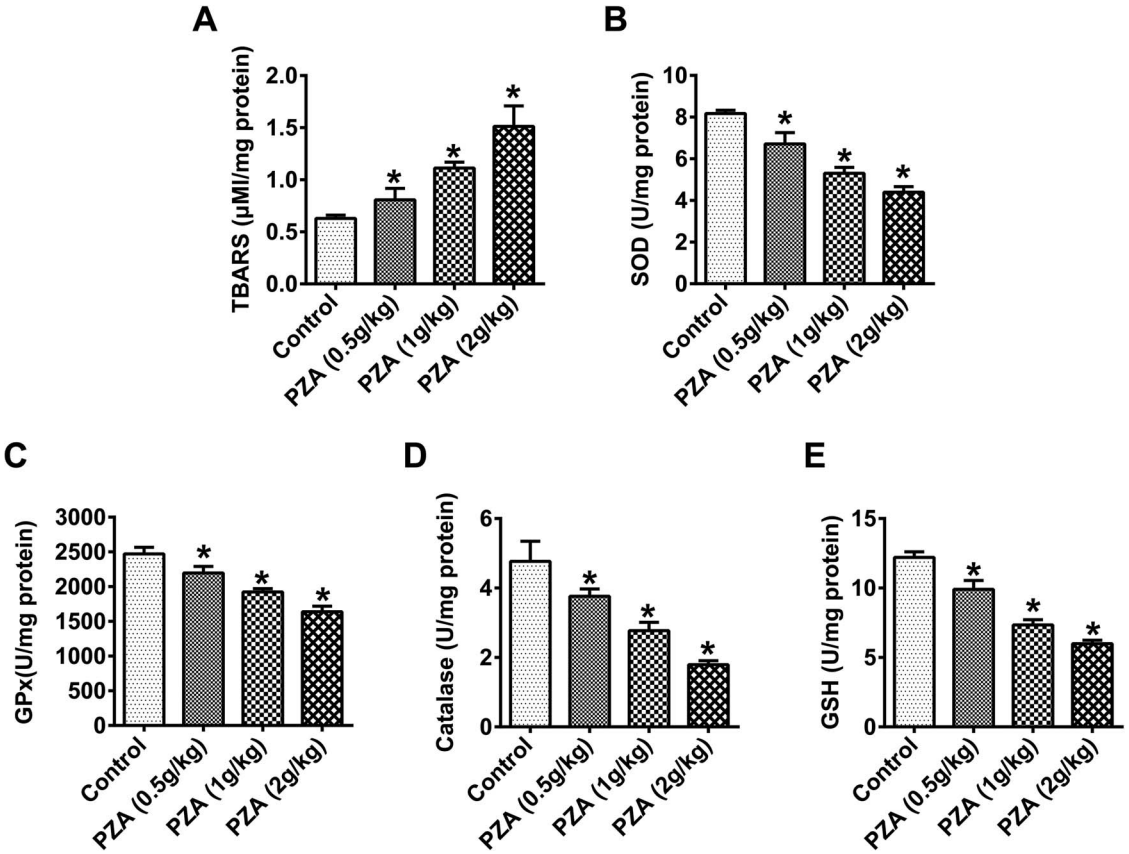

Figure 2: PZA enhances lipid peroxidation and inhibits the antioxidant system of rats. Rats were orally administered 0.5 g/kg, 1 g/kg and 2 g/kg PZA for 7 days and blood samples were collected. (A) The levels of TBARS were analyzed by treatment of TBA in PZA-treated rats, $^*P < 0.05$ vs. control group. The levels of oxidative defense genes including SOD (B), GPx (C), catalase (D) and GSH (E) were detected using commercial kits in PZA-treated rats, $^*P < 0.05$ vs. control group.

treatment groups compared to controls ($P < 0.05$), indicating that PZA inhibits PI3K/Akt signaling.

Activation of PI3K/Akt by 740Y-P attenuates PZA-induced liver injury in rats

To confirm whether PZA promotes liver injury through its ability to regulate PI3K/Akt signaling, PZA-induced rats were treated with the PI3K activator (740Y-P). Western blot assays showed that PZA-induced p-PI3K and p-Akt inhibition were reversed by 740Y-P treatment ($P < 0.05$, Fig. 5A). PZA-mediated increases in ALT, AST, γ-GT and TBIL levels were also significantly inhibited by 740Y-P ($P < 0.05$, Fig. 5B and E). H&E staining showed that PZA-mediated liver injury including liver cell edema, inflammatory cell infiltration and ballooning degeneration were alleviated by 740Y-P treatment (Fig. 5F). This revealed that PI3K activation could alleviate liver injury in rats in response to PZA.

740Y-P prevents PZA-induced alterations in lipid peroxidation and the antioxidant system

We next analyzed whether 740Y-P reverses PZA-mediated alterations in lipid peroxidation and the antioxidant system. Rats induced by PZA were treated with 740Y-P and blood samples were collected. Lipid peroxidation (TBARS) was significantly decreased in PZA + 740Y-P groups compared to PZA + vehicle groups in rat livers, suggesting that 740Y-P could reduce the levels of TBARS in response to PZA in rats ($P < 0.05$, Fig. 6A). We further confirmed that the levels of SOD, GPx, catalase and GSH were significantly increased in PZA + 740Y-P groups with respect to PZA + vehicle groups in the rat liver, indicating that 740Y-P could accelerate antioxidant responses that were prevented by PZA in rats ($P < 0.05$, Figure 6B and E).

740Y-P attenuates PZA-induced apoptosis in rat liver tissue

We next investigated whether 740Y-P could reverse PZA-mediated apoptosis in the liver tissues of rats. TUNEL staining showed that PZA-induced apoptosis in liver tissues was significantly alleviated by 740Y-P treatment ($P < 0.05$, Fig. 7A). Western blot analyses also indicated that Bcl-2 expression was significantly upregulated, whereas Bax and caspase-3 expression were downregulated in the 740Y-P group compared to vehicle groups in PZA-treated rat livers ($P < 0.05$, Fig. 7B). Accordingly, we these data confirmed that PZA enhanced apoptosis in rat livers through PI3K/Akt activation.

Discussion

Although PI3K/Akt mediated regulation of gene expression regulates lipid and glucose metabolism [33], inflammation [34], ROS [35], fatty acid oxidation [36] and adipocyte differentiation [37] its role in liver injury induced by PZA is unclear. The aim of this study was to further clarify the mechanism of liver injury

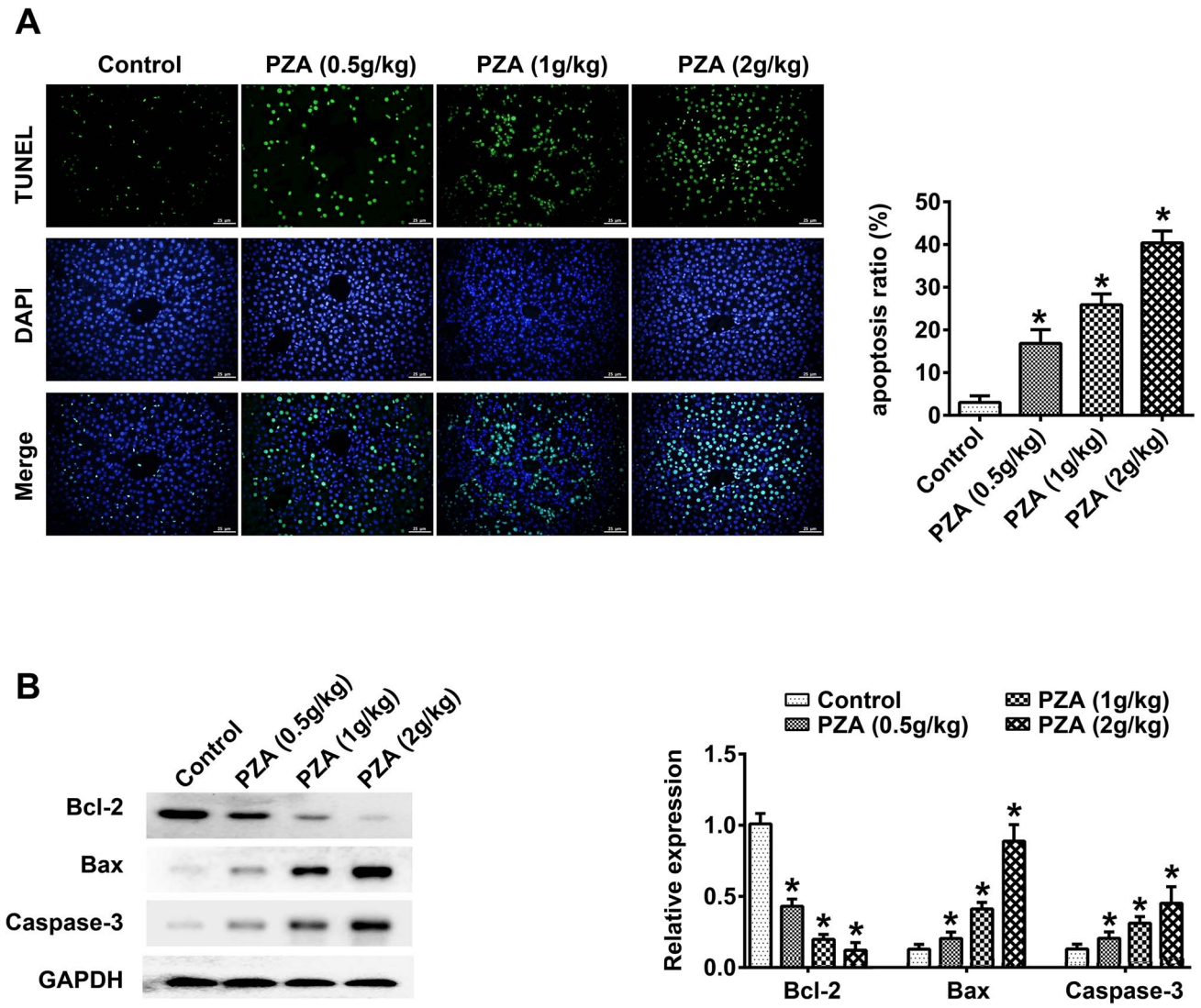

Figure 3: PZA promotes apoptosis in rat livers. Rats were also orally administered 0.5 g/kg, 1 g/kg and 2 g/kg PZA for 7 days. (A) Apoptosis in rat livers was confirmed by TUNEL staining. Magnification, ×200, scale bar = 25 μm. The number of apoptotic cells were quantified, $^{*}P < 0.05$ vs. control group. (B) Western blot analysis of Bcl-2, Bax and caspase-3 in PZA-treated rats normalized to GAPDH. Values were quantitated according to the gray values, $^{*}P < 0.05$ vs. control group.

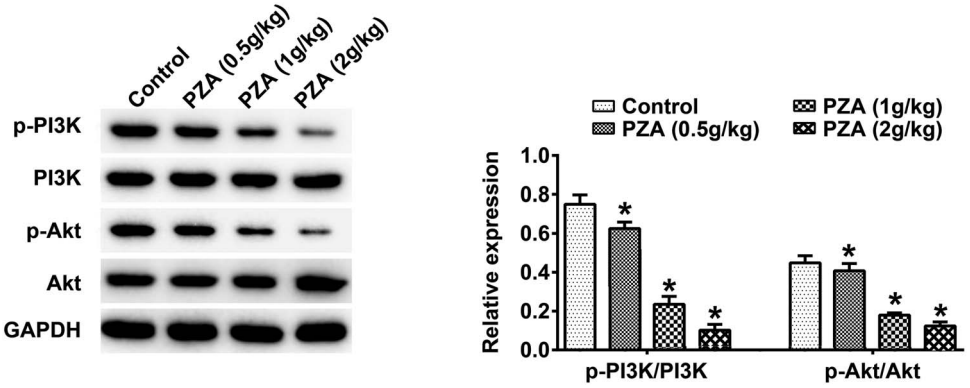

Figure 4: PZA downregulates the expression of PI3K/Akt in rat liver. Effects of PZA on PI3K, p-PI3K, Akt and p-Akt expression assessed by western blot analysis in the liver tissues of rats treated with 0.5 g/kg, 1 g/kg and 2 g/kg PZA. Protein levels were quantitatively analyzed, $^{*}P < 0.05$ vs. control group.

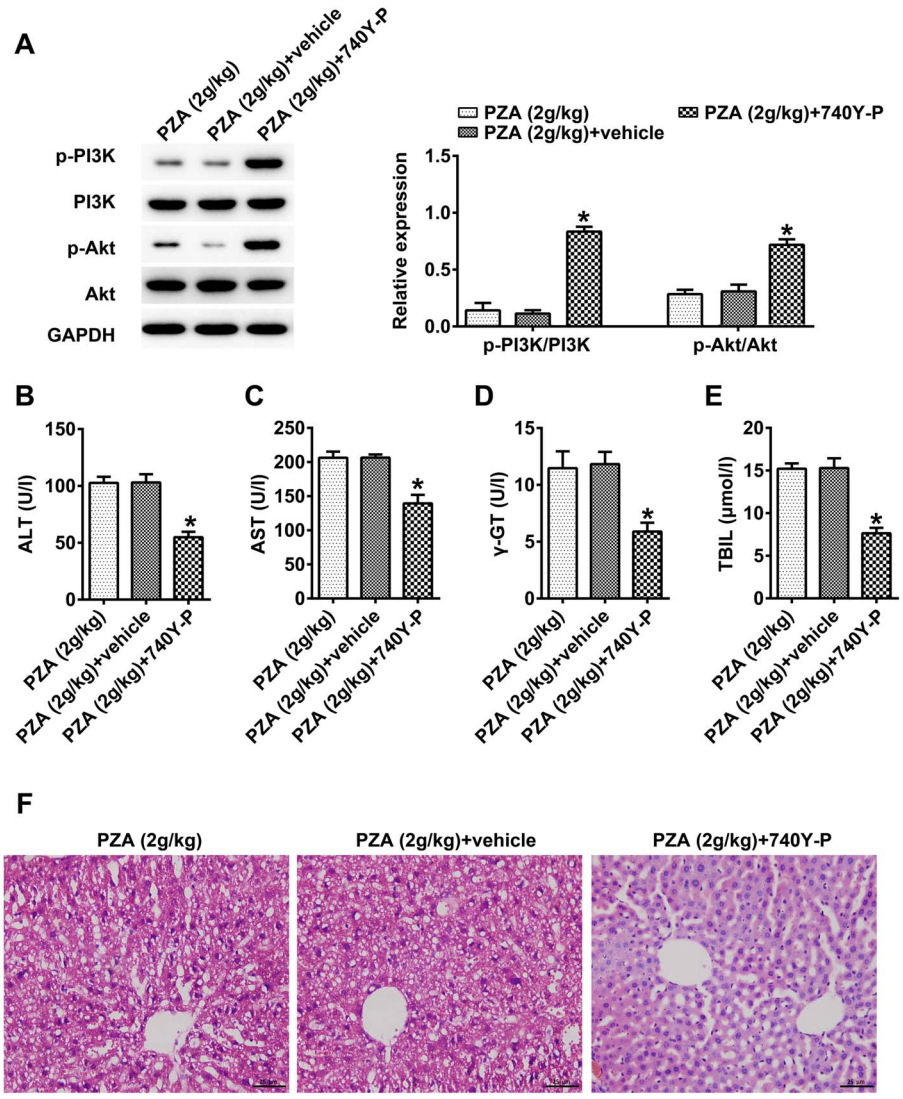

Figure 5: Activation of PI3K/Akt signaling is attenuated by 740Y-P treatment in PZA-induced rat liver injury models. Rats were treated with 2 g/kg PZA and 740Y-P, respectively. (A) Western blot analysis of PI3K, p-PI3K, Akt and p-Akt expression in PZA and 740Y-P-treated rats. Quantitative analyses of the PI3K/Akt pathway. *$P < 0.05$ vs. PZA + vehicle group. Influence of 740Y-P on the levels of ALT (B), AST (C), γ-GT (D), TBIL (E) were evaluated in PZA-treated rats, *$P < 0.05$ vs. PZA + vehicle group. (F) Effects of 740Y-P on the pathological status of liver injury assessed by H&E staining in PZA-treated rats. Magnification, ×200, scale bar = 25 μm.

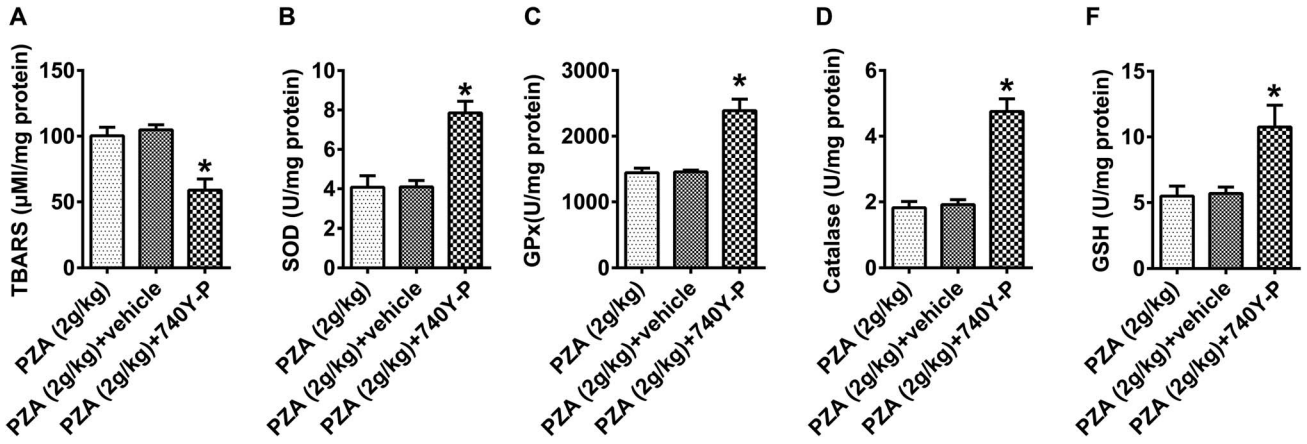

Figure 6: 740Y-P weakens PZA-induced alterations in lipid peroxidation and antioxidant defenses. Concentration of TBARS (A), SOD (B), GPx (C), catalase (D) and GSH (E) assessed in PZA and 740Y-P-treated rats, *$P < 0.05$ vs. PZA + vehicle group.

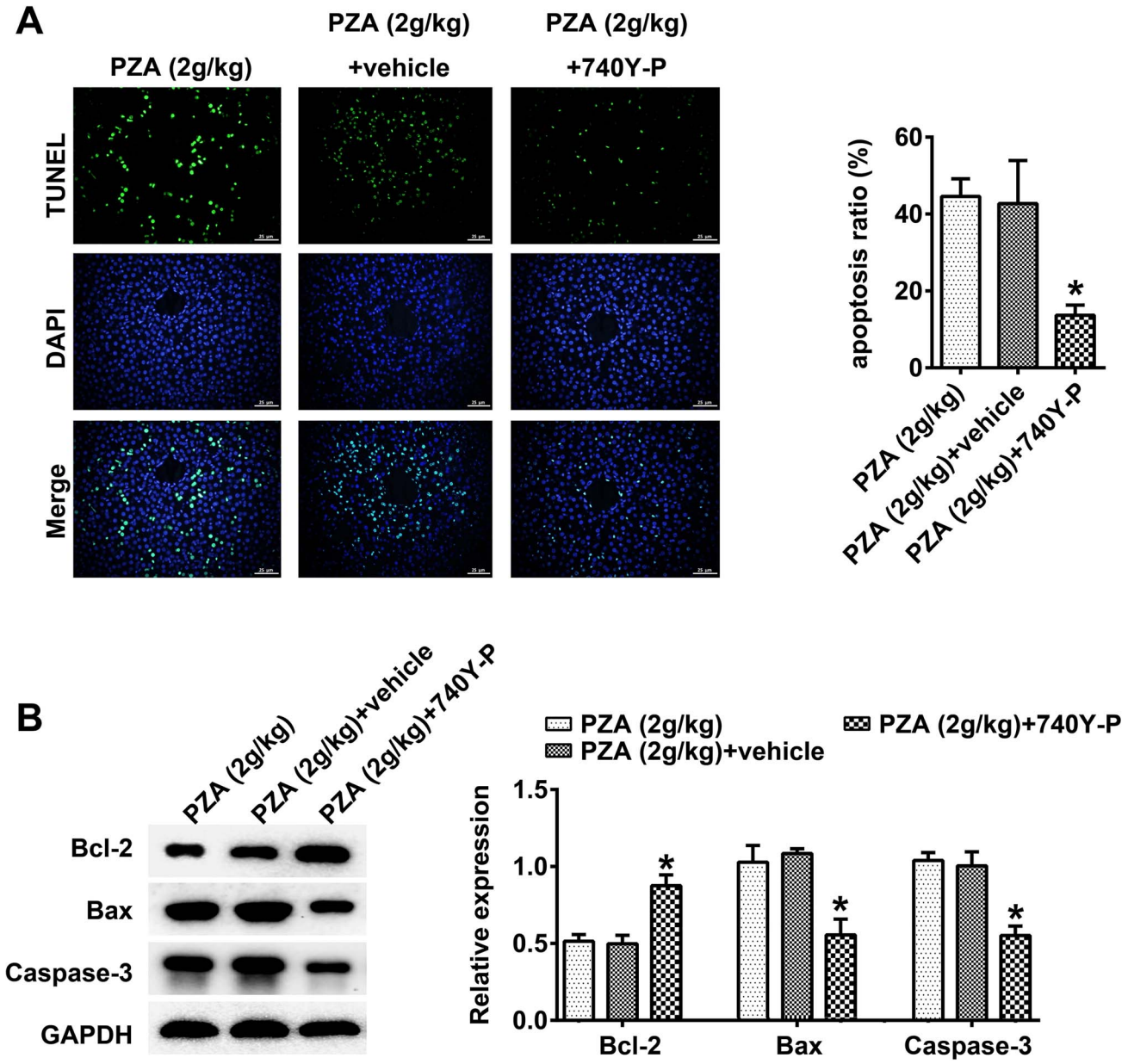

Figure 7: 740Y-P attenuates PZA-induced apoptosis in the liver tissues of rats. (A) Following treatment with 2 g/kg PZA and 740Y-P, apoptosis was examined by TUNEL staining. Magnification, ×200, scale bar = 25 μm. Apoptosis was quantitatively analyzed, $^{*}P < 0.05$ vs. PZA + vehicle group. (B) Western blot analysis of apoptosis-associated proteins in the liver tissues of PZA and 740Y-P-treated rats. Relative expression levels were quantified. $^{*}P < 0.05$ vs. PZA + vehicle group.

induced by PZA. The key findings of this study were that PZA induces liver injury, enhances lipid peroxidation and apoptosis and inhibits antioxidant defenses in a dose-dependent manner. PZA also dramatically inhibited PI3K and Akt phosphorylation in rat livers and the influence of PZA on liver injury could be attenuated by PI3K/Akt activation.

Histopathological observations of the liver are the gold standard for evaluating the degree of liver injury, which is widely employed in many animal models of liver injury [38]. ALT, AST, γ-GT and TBIL are the most sensitive indices to reflect liver function [39]. In this study, PZA markedly increased ALT, AST, γ-GT and TBIL levels in a dose-dependent manner. In addition, histological results revealed that the liver showed edema, inflammatory cell infiltration and balloon degeneration after PZA treatment, the severity of which increased at higher concentrations.

The hallmark of liver disease is lipid accumulation, which leads to the formation of lipid droplets in liver cells. This accumulation is caused by an imbalance between lipid synthesis and oxidation [40]. Compared to healthy patients, patients with liver disease show high levels of ROS and lipid peroxidation products, while the expressions of antioxidant enzymes such as SOD, CAT and GSH, were reduced [41, 42]. OS refers to the imbalance caused by excess ROS over the effective antioxidant capacity of cells [43]. ROS induction induces cells into a state of OS, accompanied by hepatocyte apoptosis that plays a key role in liver injury [44]. In this study, we demonstrated that PZA could enhance lipid peroxidation (TBARS) and decrease the levels of

SOD, GPx, catalase and GSH in rats in a dose-dependent manner. In addition, PZA could markedly promote apoptosis in rat livers highlighting its ability to promote liver damage.

ROS can directly interact with key signaling molecules, including PI3K and Akt to initiate signal transmission in various cellular processes [45]. Moreover, PI3K/Akt signaling is crucial to protect the body against various stimuli [46]. The activation of this pathway did not affect cell apoptosis, survival or proliferation through the regulation of downstream factors, such as apoptotic proteins Bax, Bcl-2, caspases and nuclear transcription factor κ (NF-κB) [47, 48]. The PI3K/Akt pathway is related to hepatic lipid metabolism, acute liver failure, liver ischemia/reperfusion injury, liver fibrosis and liver cancer [26, 49–52]. In this study, we further demonstrated that the activation of the PI3K/Akt pathway by 740Y-P could attenuate changes in serum indicators, histopathology, lipid peroxidation, antioxidant systems and liver apoptosis mediated by PZA. We therefore verified that PZA could accelerate liver damage through its ability to regulate PI3K/Akt signaling.

Conclusions

In this study, we identified that PZA could alter the pathological structure of the liver, promote lipid peroxidation and apoptosis and inhibit the antioxidant capacity of liver cells. More importantly, we demonstrated that the changes induced by PZA in rat livers could be markedly weakened by the PI3K activator (740Y-P). We therefore provide new evidence that furthers our molecular understanding of liver injury induced by PZA to predict drug hepatotoxicity. In addition, we provide evidence for the rational use of PZA in clinical practice. We now aim to study the influence of both upstream and downstream genes of the PI3K/Akt pathway on PZA-induced liver injury in future studies. Besides, we will also focus on the long-term low-dose treatment of PZA in the liver injury model.

Acknowledgements

This research was financially supported by the grant from the Keynote Research and Development Program of Hunan (2017SK2055).

Conflicts of interest

None declared.

References

1. Schito M, Migliori GB, Fletcher HA *et al*. Perspectives on advances in tuberculosis diagnostics, drugs, and vaccines. *Clin Infect Dis* 2015;**61**:S102–18. doi: 10.1093/cid/civ609.
2. Mitano F, Sicsú AN, Lima MC *et al*. Discourses on short-coursetherapy for tuberculosis control. *Rev Bras Enferm* 2017;**70**:126–32. doi: 10.1590/0034-7167-2016-0463.
3. Lehloenya RJ, Dheda K. Cutaneous adverse drug reactions to anti-tuberculosis drugs: State of the art and into the future. *Expert Rev Anti Infect Ther* 2012;**10**:475–86. doi: 10.1586/eri.12.13.
4. Li Y, Zhu Y, Zhong Q *et al*. Serious adverse reactions from anti-tuberculosis drugs among 599 children hospitalized for tuberculosis. *Pediatr Infect Dis J* 2017;**36**:720–5. doi: 10.1097/inf.0000000000001532.
5. Jeong I, Park JS, Cho YJ *et al*. Drug-induced hepatotoxicity of anti-tuberculosis drugs and their serum levels. *J Korean Med Sci* 2015;**30**:167–72. doi: 10.3346/jkms.2015.30.2.167.
6. Chang TE, Huang YS, Chang CH *et al*. The susceptibility of anti-tuberculosis drug-induced liver injury and chronic hepatitis C infection: A systematic review and meta-analysis. *J Chin Med Assoc* 2018;**81**:111–8. doi: 10.1016/j.jcma.2017.10.002.
7. Lonardo A, Nascimbeni F, Maurantonio M *et al*. Nonalcoholic fatty liver disease: Evolving paradigms. *World J Gastroenterol* 2017;**23**:6571–92. doi: 10.3748/wjg.v23.i36.6571.
8. Njire M, Tan Y, Mugweru J *et al*. Pyrazinamide resistance in mycobacterium tuberculosis: Review and update. *Adv Med Sci* 2016;**61**:63–71. doi: 10.1016/j.advms.2015.09.007.
9. Chirehwa MT, McIlleron H, Rustomjee R *et al*. Pharmacokinetics of pyrazinamide and optimal dosing regimens for drug-sensitive and -resistant tuberculosis. *Antimicrob Agents Chemother* 2017;**61**. doi: 10.1128/aac.00490-17.
10. Hu Y, Coates AR, Mitchison DA. Sterilising action of pyrazinamide in models of dormant and rifampicin-tolerant mycobacterium tuberculosis. *Inte J Tuberculosis Lung Dis* 2006;**10**:317–22.
11. Correa MF, Fernandes JP. Pyrazinamide and Pyrazinoic acid derivatives directed to mycobacterial enzymes against tuberculosis. *Curr Protein Pept Sci* 2016;**17**:213–9.
12. Duru CB, Uwakwe KA, Nnebue CC *et al*. Tuberculosis treatment outcomes and determinants among patients treated in hospitals in Imo state, Nigeria. *Open Access Library J* 2016;**3**:e2754.
13. Horita N, Miyazawa N. [drug-induced liver injury and pyrazinamide use]. *Kekkaku : [Tuberculosis]* 2015;**90**:401–5.
14. Guo HL, Hassan HM, Zhang Y *et al*. Pyrazinamide induced rat cholestatic liver injury through inhibition of FXR regulatory effect on bile acid synthesis and transport. *Toxicol Sci* 2016;**152**:417–28. doi: 10.1093/toxsci/kfw098.
15. El-Boshy ME, Risha EF, Abdelhamid FM *et al*. Protective effects of selenium against cadmium induced hematological disturbances, immunosuppressive, oxidative stress and hepatorenal damage in rats. *J Trace Elem Med Biol* 2015;**29**:104–10. doi: 10.1016/j.jtemb.2014.05.009.
16. Paradies G, Paradies V, Ruggiero FM *et al*. Oxidative stress, cardiolipin and mitochondrial dysfunction in nonalcoholic fatty liver disease. *World J Gastroenterol* 2014;**20**:14205–18. doi: 10.3748/wjg.v20.i39.14205.
17. Wang K. Autophagy and apoptosis in liver injury. *Cell Cycle* 2015;**14**:1631–42. doi: 10.1080/15384101.2015.1038685.
18. Shehu AI, Ma X, Venkataramanan R. Mechanisms of drug-induced hepatotoxicity. *Clin Liver Dis* 2017;**21**:35–54. doi: 10.1016/j.cld.2016.08.002.
19. Goncalves MD, Hopkins BD, Cantley LC. Phosphatidylinositol 3-kinase, growth disorders, and cancer. *N Engl J Med* 2018;**379**:2052–62. doi: 10.1056/NEJMra1704560.
20. Di Blasio L, Gagliardi PA, Puliafito A *et al*. Serine/threonine kinase 3-Phosphoinositide-dependent protein Kinase-1 (PDK1) as a key regulator of cell migration and cancer dissemination. *Cancer* 2017;**9**. doi: 10.3390/cancers9030025.
21. Vergadi E, Ieronymaki E, Lyroni K *et al*. Akt Signaling pathway in macrophage activation and M1/M2 polarization. *J Immunol* 2017;**198**:1006–14. doi: 10.4049/jimmunol.1601515.
22. Fresno Vara JA, Casado E, de Castro J *et al*. PI3K/Akt signalling pathway and cancer. *Cancer Treat Rev* 2004;**30**:193–204. doi: 10.1016/j.ctrv.2003.07.007.
23. O'Donnell JS, Massi D, Teng MWL *et al*. PI3K-AKT-mTOR inhibition in cancer immunotherapy, redux. *Semin Cancer Biol* 2018;**48**:91–103. doi: 10.1016/j.semcancer.2017.04.015.

24. Xu S, Wu L, Zhang Q *et al*. Pretreatment with propylene glycol alginate sodium sulfate ameliorated concanavalin A-induced liver injury by regulating the PI3K/Akt pathway in mice. *Life Sci* 2017;**185**:103–13. doi: 10.1016/j.lfs.2017.07.033.
25. Yao Y, Wang L, Jin P *et al*. Methane alleviates carbon tetrachloride induced liver injury in mice: Anti-inflammatory action demonstrated by increased PI3K/Akt/GSK-3beta-mediated IL-10 expression. *J Mol Histol* 2017;**48**:301–10. doi: 10.1007/s10735-017-9728-1.
26. Zhang Y, Wei Z, Liu W *et al*. Melatonin protects against arsenic trioxide-induced liver injury by the upregulation of Nrf2 expression through the activation of PI3K/AKT pathway. *Oncotarget* 2017;**8**:3773–80. doi: 10.18632/oncotarget.13931.
27. Zhang Y, Hongli G, Hassan HM *et al*. Pyrazinamide induced hepatic injury in rats through inhibiting the PPARα pathway. *J Appl Toxicol* 2016;**36**:1579–90.
28. Ghani MA, Barril C, Bedgood DR Jr *et al*. Measurement of antioxidant activity with the thiobarbituric acid reactive substances assay. *Food Chem* 2017;**230**:195–207. doi: 10.1016/j.foodchem.2017.02.127.
29. Dikalov SI, Harrison DG. Methods for detection of mitochondrial and cellular reactive oxygen species. *Antioxid Redox Signal* 2014;**20**:372–82. doi: 10.1089/ars.2012.4886.
30. Deshpande KC, Kulkarni MM, Rajput DV. Evaluation of glutathione peroxidase in the blood and tumor tissue of oral squamous cell carcinoma patients. *J Oral Maxillofac Pathol* 2018;**22**:447. doi: 10.4103/jomfp.JOMFP_140_17.
31. Radi, R. Turrens J.F., Chang L.Y. *et al*. Detection of catalase in rat heart mitochondria. *J Biol Chem* 1991;**266**:22028–34.
32. Huang J, Jia Y, Li Q *et al*. Glutathione content and expression of proteins involved with glutathione metabolism differs in longissimus dorsi, subcutaneous adipose, and liver tissues of finished vs. growing beef steers. *J Anim Sci* 2018;**96**:5152–65. doi: 10.1093/jas/sky362.
33. Cui X, Qian DW, Jiang S *et al*. Scutellariae radix and Coptidis Rhizoma improve glucose and lipid metabolism in T2DM rats via regulation of the metabolic profiling and MAPK/PI3K/Akt Signaling pathway. *Int J Mol Sci* 2018;**19**. doi: 10.3390/ijms19113634.
34. Xue JF, Shi ZM, Zou J *et al*. Inhibition of PI3K/AKT/mTOR signaling pathway promotes autophagy of articular chondrocytes and attenuates inflammatory response in rats with osteoarthritis. *Biomed Pharmacother* 2017;**89**:1252–61. doi: 10.1016/j.biopha.2017.01.130.
35. Zha, L. Chen J., Sun S. *et al*. Soyasaponins can blunt inflammation by inhibiting the reactive oxygen species-mediated activation of PI3K/Akt/NF-kB pathway. *PLoS One* **9**, e107655, doi:10.1371/journal.pone.0107655 (2014).
36. Pisonero-Vaquero S, Martínez-Ferreras Á, García-Mediavilla MV *et al*. Quercetin ameliorates dysregulation of lipid metabolism genes via the PI3K/AKT pathway in a diet-induced mouse model of nonalcoholic fatty liver disease. *Mol Nutr Food Res* 2015;**59**:879–93. doi: 10.1002/mnfr.201400913.
37. Song BQ, Chi Y, Li X *et al*. Inhibition of notch signaling promotes the Adipogenic differentiation of mesenchymal stem cells through autophagy activation and PTEN-PI3K/AKT/mTOR pathway. *Cell Physiol Biochem* 2015;**36**:1991–2002. doi: 10.1159/000430167.
38. Chai L, Chen A, Luo P *et al*. Histopathological changes and lipid metabolism in the liver of *Bufo gargarizans* tadpoles exposed to Triclosan. *Chemosphere* 2017;**182**:255–66. doi: 10.1016/j.chemosphere.2017.05.040.
39. Tang N, Zhang Y, Liu Z *et al*. Correlation analysis between four serum biomarkers of liver fibrosis and liver function in infants with cholestasis. *Biomed Rep* 2016;**5**:107–12. doi: 10.3892/br.2016.681.
40. Carr RM, Ahima RS. Pathophysiology of lipid droplet proteins in liver diseases. *Exp Cell Res* 2016;**340**:187–92. doi: 10.1016/j.yexcr.2015.10.021.
41. Cichoz-Lach H, Michalak A. Oxidative stress as a crucial factor in liver diseases. *World J Gastroenterol* 2014;**20**:8082–91. doi: 10.3748/wjg.v20.i25.8082.
42. Liu W, Baker SS, Baker RD *et al*. Antioxidant mechanisms in nonalcoholic fatty liver disease. *Curr Drug Targets* 2015;**16**:1301–14.
43. Sies H. Oxidative stress: a concept in redox biology and medicine. *Redox Biol* 2015;**4**:180–3. doi: 10.1016/j.redox.2015.01.002.
44. Du X, Shi Z, Peng Z *et al*. Acetoacetate induces hepatocytes apoptosis by the ROS-mediated MAPKs pathway in ketotic cows. *J Cell Physiol* 2017;**232**:3296–308. doi: 10.1002/jcp.25773.
45. Zhang J, Wang X, Vikash V *et al*. ROS and ROS-mediated cellular signaling. *Oxid Med Cell Longev* 2016;**2016**:4350965. doi: 10.1155/2016/4350965.
46. Mayer IA, Arteaga CL. The PI3K/AKT pathway as a target for cancer treatment. *Annu Rev Med* 2016;**67**:11–28. doi: 10.1146/annurev-med-062913-051343.
47. Wang T, Gong X, Jiang R *et al*. Ferulic acid inhibits proliferation and promotes apoptosis via blockage of PI3K/Akt pathway in osteosarcoma cell. *Am J Translat Res* 2016;**8**:968–80.
48. Chai R, Fu H, Zheng Z *et al*. Resveratrol inhibits proliferation and migration through SIRT1 mediated posttranslational modification of PI3K/AKT signaling in hepatocellular carcinoma cells. *Mol Med Rep* 2017;**16**:8037–44. doi: 10.3892/mmr.2017.7612.
49. El-Mihi KA, Kenawy HI, El-Karef A *et al*. Naringin attenuates thioacetamide-induced liver fibrosis in rats through modulation of the PI3K/Akt pathway. *Life Sci* 2017;**187**:50–7. doi: 10.1016/j.lfs.2017.08.019.
50. Li H, Chen O, Ye Z *et al*. Inhalation of high concentrations of hydrogen ameliorates liver ischemia/reperfusion injury through A2A receptor mediated PI3K-Akt pathway. *Biochem Pharmacol* 2017;**130**:83–92. doi: 10.1016/j.bcp.2017.02.003.
51. Li Y, Lu L, Luo N *et al*. Inhibition of PI3K/AKt/mTOR signaling pathway protects against d-galactosamine/lipopolysaccharide-induced acute liver failure by chaperone-mediated autophagy in rats. *Biomed Pharmacother* 2017;**92**:544–53. doi: 10.1016/j.biopha.2017.05.037.
52. Liao X, Song L, Zhang L *et al*. LAMP3 regulates hepatic lipid metabolism through activating PI3K/Akt pathway. *Mol Cell Endocrinol* 2018;**470**:160–7. doi: 10.1016/j.mce.2017.10.010.